The Plant Cell, Vol. 27: 3321–3335, December 2015, www.plantcell.org

The ASYMMETRIC LEAVES Complex Employs Multiple Modes of Regulation to Affect Adaxial-Abaxial Patterning and Leaf Complexity[OPEN]

Aman Y. Husbands,[a] Anna H. Benkovics,[a] Fabio T.S. Nogueira,[a,1] Mukesh Lodha,[a,2] and Marja C.P. Timmermans[a,b,3]

[a] Cold Spring Harbor Laboratory, Cold Spring Harbor, New York 11724
[b] Center for Plant Molecular Biology, University of Tübingen, 72076 Tuebingen, Germany

Flattened leaf architecture is not a default state but depends on positional information to precisely coordinate patterns of cell division in the growing primordium. This information is provided, in part, by the boundary between the adaxial (top) and abaxial (bottom) domains of the leaf, which are specified via an intricate gene regulatory network whose precise circuitry remains poorly defined. Here, we examined the contribution of the ASYMMETRIC LEAVES (AS) pathway to adaxial-abaxial patterning in *Arabidopsis thaliana* and demonstrate that AS1-AS2 affects this process via multiple, distinct regulatory mechanisms. AS1-AS2 uses Polycomb-dependent and -independent mechanisms to directly repress the abaxial determinants *MIR166A*, *YABBY5*, and *AUXIN RESPONSE FACTOR3* (*ARF3*), as well as a nonrepressive mechanism in the regulation of the adaxial determinant *TAS3A*. These regulatory interactions, together with data from prior studies, lead to a model in which the sequential polarization of determinants, including AS1-AS2, explains the establishment and maintenance of adaxial-abaxial leaf polarity. Moreover, our analyses show that the shared repression of *ARF3* by the AS and *trans*-acting small interfering RNA (ta-siRNA) pathways intersects with additional AS1-AS2 targets to affect multiple nodes in leaf development, impacting polarity as well as leaf complexity. These data illustrate the surprisingly multifaceted contribution of AS1-AS2 to leaf development showing that, in conjunction with the ta-siRNA pathway, AS1-AS2 keeps the Arabidopsis leaf both flat and simple.

INTRODUCTION

The formation of a stable, precisely defined boundary between two distinct cell fates is a fundamental feature of plant and animal development. Such cell fate boundaries coordinate the further patterning and growth of the tissue or organ. Accordingly, failure to maintain a stable cell fate boundary can result in dramatic developmental defects. Likewise, adaxial-abaxial leaf polarity, which directs the acquisition of distinct cell fates within the leaf's adaxial/top and abaxial/bottom domains, must be carefully controlled. The boundary between these domains drives the flattened outgrowth of the leaf (Waites and Hudson, 1995), and slight perturbations in either adaxial or abaxial identity cause progressive leaf curling with severe consequences for physiological function (Lang et al., 2004; Zhang et al., 2009; Nakata et al., 2012). Adaxial-abaxial leaf polarity in particular poses an unusual and mechanistically challenging problem, namely, how to create a stable boundary within the plane of a long and wide, but shallow, structure. This requires precise coordination of division and differentiation patterns for hundreds of cells throughout primordium development.

The acquisition and maintenance of adaxial-abaxial polarity are driven by a complex, redundant gene regulatory network with several highly conserved transcription factor families that promote either adaxial or abaxial fate at its core (reviewed in Husbands et al., 2009; Moon and Hake, 2011). Members of the CLASS III HOMEODOMAIN-LEUCINE ZIPPER (HD-ZIPIII) family, which in *Arabidopsis thaliana* includes *PHABULOSA* (*PHB*), *PHAVOLUTA*, and *REVOLUTA* (*REV*), specify adaxial cell fate (McConnell et al., 2001; Emery et al., 2003; Juarez et al., 2004). In addition, the Myb domain transcription factor ASYMMETRIC LEAVES1 (AS1) promotes adaxial identity in complex with the LATERAL ORGAN BOUNDARIES domain transcription factor AS2 (Lin et al., 2003; Husbands et al., 2007; Iwakawa et al., 2007). By contrast, members of the KANADI (KAN) and YABBY (YAB) gene families, along with *AUXIN RESPONSE FACTOR3* (*ARF3*) and *ARF4*, contribute to the specification of abaxial cell fate (Siegfried et al., 1999; Eshed et al., 2001; Kerstetter et al., 2001; Pekker et al., 2005).

The two sets of transcription factors are expressed in complementary domains on the top and bottom side of the leaf, respectively. The positional information needed to delineate these domains is provided in part by the small RNAs miR166 and tasiR-ARF. The latter is generated through a specialized *trans*-acting small interfering RNA (ta-siRNA) pathway. In Arabidopsis, this pathway employs a dedicated miR390-ARGONAUTE7 (AGO7) complex to target *TAS3A* transcripts, which are then made

[1] Current address: Centro de Biotecnologia Agricola, Escola Superior de Agricultura Luiz de Queiroz, University of Sao Paulo, Piracicaba, Sao Paulo, Brazil.
[2] Current address: Centre for Cellular and Molecular Biology, Uppal Road, Hyderabad-500 007, India.
[3] Address correspondence to timmerma@cshl.edu.
The author responsible for distribution of materials integral to the findings presented in this article in accordance with the policy described in the Instructions for Authors (www.plantcell.org) is: Marja C.P. Timmermans (timmerma@cshl.edu).
[OPEN]Articles can be viewed online without a subscription.
www.plantcell.org/cgi/doi/10.1105/tpc.15.00454

double-stranded through the action of SUPPRESSOR OF GENE SILENCING3 and RNA-DEPENDENT RNA POLYMERASE6. These double-stranded RNAs are subsequently processed by DICER-LIKE4 into 21-nucleotide phased small RNAs, a subset of which, the tasiR-ARFs, go on to regulate *ARF3* and *ARF4* (reviewed in Chapman and Carrington, 2007). Importantly, while tasiR-ARF biogenesis is restricted to the two adaxial-most cell layers of developing primordia, movement of these small RNAs creates an abaxially dissipating gradient that through a possible dose-dependent readout limits expression of the ARF3 and ARF4 targets to the bottom side of leaf primordia (Chitwood et al., 2009; Skopelitis et al., 2012). Likewise, miR166 forms a gradient across the developing leaf, but this gradient has its maximum on the abaxial side (Juarez et al., 2004; Nogueira et al., 2007; Yao et al., 2009). miR166 guides the cleavage of HD-ZIPIII transcripts, limiting expression of these adaxial determinants to the top side of primordia (McConnell et al., 2001; Emery et al., 2003; Juarez et al., 2004).

In addition to the opposing activities of these small RNAs, the transcription factors at the center of the adaxial-abaxial polarity network are characterized by mutually antagonistic behavior (Waites and Hudson, 1995; Kerstetter et al., 2001; Eshed et al., 2001; Emery et al., 2003). This leads to mutual exclusivity of adaxial versus abaxial cell fates and contributes to clean separation at the domain level (Husbands et al., 2009). While mutual antagonism between polarity determinants was inferred from early genetic studies, the mechanistic basis for this remains largely unknown. The recent finding that the HD-ZIPIII and KAN proteins act oppositely on a common set of targets (Merelo et al., 2013; Reinhart et al., 2013; Huang et al., 2014) suggests one possible mechanism by which mutual antagonism may occur. However, the clean separation of cell fates and maintenance of a stable boundary likely requires a more immediate and direct mechanism. This could be achieved by direct repressive interactions between the polarity determinants themselves, for example, the direct repression of *AS2*, and possibly *PHB*, by KAN1 (Wu et al., 2008; Huang et al., 2014).

Ironically, mutual antagonism makes identifying such direct interactions between the transcription factors at the core of the polarity network more difficult, as the direct contributions of a given adaxial or abaxial determinant are not easily untangled from indirect effects related to general imbalances in the polarity network. Further compounding this, most polarity determinants have roles in development outside of adaxial-abaxial patterning. For instance, *ARF3* and *ARF4* act as repressors of the auxin-signaling network that affects a wide range of developmental processes (Fahlgren et al., 2006; Hunter et al., 2006; Marin et al., 2010). Likewise, AS1-AS2 maintains the stable silencing of meristem fate-promoting KNOX genes in developing primordia (Guo et al., 2008; Lodha et al., 2013). Specifically, AS1-AS2 was shown to bind discrete *cis*-elements in the promoters of *BREVIPEDICELLUS* (*BP*) and *KNAT2*, leading to recruitment of Polycomb complexes that stably repress KNOX gene expression in determinant cells. Such a silencing mechanism would fit within the established paradigm of mutual antagonism between adaxial and abaxial determinants.

With this in mind, we set out to map the contributions of the Arabidopsis AS pathway to adaxial fate acquisition using complementary biochemical and genetic approaches. We show that AS1-AS2 binds the promoters of both adaxial and abaxial determinants and exploits distinct mechanisms to regulate target activity. AS1-AS2 employs both Polycomb-dependent and -independent mechanisms to directly repress activity of the abaxial determinants *MIR166A*, *YAB5*, and *ARF3* and further uses a nonrepressive, possibly protective, mechanism in the regulation of *TAS3A* on the adaxial side. These regulatory interactions, together with data from prior studies, suggest a model in which the sequential polarization of polarity determinants, including AS1-AS2, explains the establishment and maintenance of adaxial-abaxial leaf polarity. Moreover, our analyses show that the shared repression of *ARF3* by the AS and ta-siRNA pathways intersects with additional AS1-AS2 targets to affect multiple nodes in leaf development. Loss of *ARF3* regulation by mutation of both the AS and ta-siRNA pathways leads to enhanced abaxialized defects reflecting the loss of multiple adaxial-promoting factors. Double mutants also show a dramatic and unexpected reduction in *TAS3A* transcript levels, predicting the presence of a feedback loop in which targets of tasiR-ARF, in conjunction with AS1-AS2 binding at the promoter of *TAS3A*, polarize tasiR-ARF biogenesis. Finally, the AS and ta-siRNA pathways converge to suppress leaf complexity via the specific activity of ARF3, a function that is not shared by ARF4. These data illustrate the surprisingly multifaceted contribution of AS1-AS2 to leaf development showing that, in conjunction with the ta-siRNA pathway, AS1-AS2 keeps the Arabidopsis leaf both flat and simple.

RESULTS

AS1-AS2 Directly Regulates Adaxial-Abaxial Polarity Determinants

To better understand the molecular basis for the mutual exclusivity of adaxial and abaxial cell fates, we set out to define the role AS1 and AS2 play in regulating adaxial-abaxial polarity. These transcription factors have been shown to bind *cis*-regulatory elements with consensus sequences CWGTTD (Motif I) and KMKTTGAHW (Motif II) in the promoters of *BP* and *KNAT2* (Guo et al., 2008), prompting us to scan for similar sequence motifs in the regulatory regions of key polarity determinants. Putative AS1-AS2 targets were selected based on adherence to the following criteria: First, putative targets must include both Motifs I and II, but as the consensus sequences for these AS1-AS2 binding elements are based on data from just two targets, specifications for these motifs were relaxed to be as inclusive as possible of putative targets. As such, Motif I became CNGTTD, the consensus Myb binding site and, in line with most known plant transcription factor binding motifs (Franco-Zorrilla et al., 2014), Motif II was reduced to the core element KTTGAH. Second, Motifs I and II must be found on the same strand of DNA, with Motif I being located upstream of Motif II. Third, as the spacing between Motifs I and II at *BP* and *KNAT2* is highly variable and the maximum functional distance between them is not known, a spacing limit of 175 nucleotides, three times the maximum distance between motifs I and II at *BP* or *KNAT2*, was used to maximize the number of potential targets. Fourth, even though AS1-AS2 occupy two pairs of binding sites in the *BP* and *KNAT2* promoters (Guo et al., 2008), polarity genes containing a single binding site comprising Motifs I and II were still considered putative targets.

Using these criteria, we identified 34 potential AS1-AS2 binding sites in the regulatory regions of 18 core components of the adaxial-abaxial polarity network (Supplemental Table 1). To assess whether the AS1-AS2 complex occupies these *cis*-elements in planta, we utilized a transgenic line expressing an estradiol-inducible translational AS2-YFP fusion (*OlexA:AS2-YFP*; Lodha et al., 2013) in chromatin immunoprecipitation (ChIP) assays. *OlexA:AS2-YFP* seedlings grown in the absence of estradiol appear completely wild-type (Supplemental Figure 1A) and show no YFP fluorescence, but upon induction with 5 μM estradiol, *OlexA:AS2-YFP* seedlings develop an adaxialized leaf phenotype and accumulate AS2-YFP RNA and protein (Supplemental Figures 1B to 1D). ChIP assays on chromatin prepared from such seedlings showed significant enrichment of AS2-YFP at binding sites in the promoters of four of the predicted AS1-AS2 targets: *ARF3*, *MIR166A*, *YAB5*, and *TAS3A* (Figure 1). ChIP analyses of mock-treated seedlings did not show this enrichment, substantiating that AS2 binds the promoters of key polarity determinants (Supplemental Figure 1F). Furthermore, consistent with data showing AS1 and AS2 operate as a complex (Lin et al., 2003; Guo et al., 2008), ChIP assays on seedlings expressing a functional AS1-HA fusion showed specific localization of AS1 to these *ARF3*, *MIR166A*, *YAB5*, and *TAS3A* promoter regions (Supplemental Figure 1E). Importantly, while a recent genome-wide analysis of AS1 activity identified *ARF3* as a potential direct target (Iwasaki et al., 2013), the binding site proposed to mediate this regulation is distinct from the AS1-AS2 target site defined here. Moreover, the presence and position of the AS1-AS2 binding site identified in this study neatly explains the observation that deletion of the proposed AS1 target site from an *ARF3:GUS* transcriptional reporter does not phenocopy its pattern of misexpression in *as1*.

Considering that AS1 and AS2 promote adaxial identity, binding of these proteins to regulatory regions of the abaxial determinants *ARF3*, *MIR166A*, and *YAB5* is conceptually consistent with the reported function of AS1-AS2 in a repressor complex and with mutual antagonism between adaxial and abaxial factors (Guo et al., 2008; Lodha et al., 2013). However, a role for AS1-AS2 in the regulation of *ARF3* will need to be more complex, as *ARF3* is transcribed throughout developing leaf primordia and only becomes polarly localized in response to tasiR-ARF activity (Chitwood et al., 2009). Moreover, AS1-AS2 also binds the promoter of *TAS3A*. Expression of this polarity determinant on the adaxial side of leaves overlaps that of *AS2* (Garcia et al., 2006; Iwakawa et al., 2007; Chitwood et al., 2009), further arguing that AS1-AS2 employs distinct mechanisms to regulate these targets.

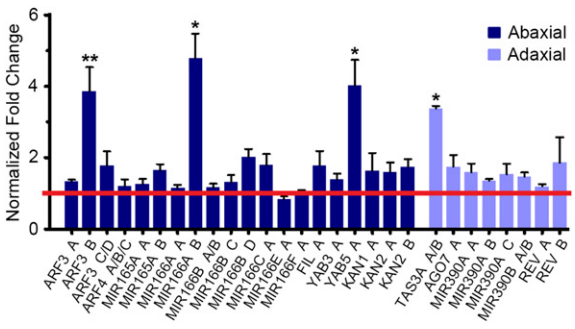

Figure 1. AS2 Binds Regulatory Regions of Key Abaxial and Adaxial Determinants.

ChIP analysis shows AS2-YFP occupies a subset of predicted AS1-AS2 binding sites in the promoters of both abaxial (dark blue) and adaxial (lavender) determinants. Significant enrichment is detected at *ARF3*, *MIR166A*, *YAB5*, and *TAS3A*. Quantitative PCR values (means ± SE) are shown as fold enrichment over the *ACT2* negative control (horizontal red line) and calculated from at least three independent biological replicates. Student's *t* test: *P < 0.05; ** P < 0.01.

Given this complexity, we sought to characterize the effect AS1-AS2 binding has on the regulation of these targets by examining expression in wild-type and *as2-4* loss-of-function mutants (Figure 2A). Transcript levels of *YAB5* and *MIR166A* are significantly increased in *as2*, suggesting that AS1-AS2 acts to repress these abaxial determinants. To substantiate this finding, we generated a *MIR166A:GUS* reporter and compared its expression in the wild type and *as2*. Consistent with previous findings (Yao et al., 2009), the *MIR166A:GUS* reporter marks the vasculature as well as the abaxial epidermis of wild-type leaf primordia (Figure 2B; Supplemental Figures 2A and 2B). While *MIR166A* expression in the vasculature is unchanged in *as2*, the *MIR166A:GUS* reporter is ectopically expressed in the rest of the blade, showing GUS activity in both the adaxial and abaxial epidermal layer of *as2* primordia (Figure 2C; Supplemental Figure 2B). Furthermore, deletion of the observed AS1-AS2 binding sites from the *MIR166A:GUS* reporter recapitulates this ectopic activity (Figure 2D). It follows that AS1-AS2 acts directly at the *MIR166A* promoter to repress transcription in the adaxial epidermis of developing leaf primordia, thereby pointing to a role for these transcription factors in polarizing the spatial distribution of miR166, which in turn delineates the expression domain of the HD-ZIPIII adaxial determinants (Emery et al., 2003). Like *MIR166A*, *YAB5* expression is restricted to the abaxial side of wild-type leaves (Iwakawa et al., 2007; Sarojam et al., 2010) and is upregulated in *as2* mutants (Figure 2A), suggesting that AS1-AS2 binding to the *YAB5* promoter may similarly contribute to the polarized activity of this abaxial determinant.

Consistent with the inference that AS1-AS2 is unlikely to act in a transcriptional repressor complex that defines the spatial expression domains of *ARF3* and *TAS3A*, transcript levels for both these targets are unchanged in *as2* leaf primordia (Figure 2A). However, formation of a normal flattened leaf requires the maintenance of a stable adaxial-abaxial boundary throughout leaf development, presenting the possibility that AS1-AS2 contributes to the temporal regulation of *ARF3* and *TAS3A* expression. To assess this possibility, we examined the effect of *as2* on the expression of the *ARF3:ARF3-GUS* reporter and *TAS3A* gene trap in older seedling leaves (Fahlgren et al., 2006; Garcia et al., 2006). *ARF3:ARF3-GUS* activity in the wild type is strongest in young primordia, where accumulation is limited to the abaxial side (Figure 2E; Chitwood et al., 2009). As the leaf matures, *ARF3:ARF3-GUS* activity subsides basipetally, with weak reporter activity persisting in the vasculature of differentiated leaves (Figures 2E and 2G). By contrast, *as2* retains *ARF3:ARF3-GUS* expression outside the vasculature, even in fully matured leaves (Figures 2E and 2H). However, as in wild-type leaf primordia, *ARF3:ARF3-GUS* reporter activity in mature *as2* leaves remains restricted to the abaxial side (Figure 2H). Thus, AS1-AS2 also functions as a repressor complex

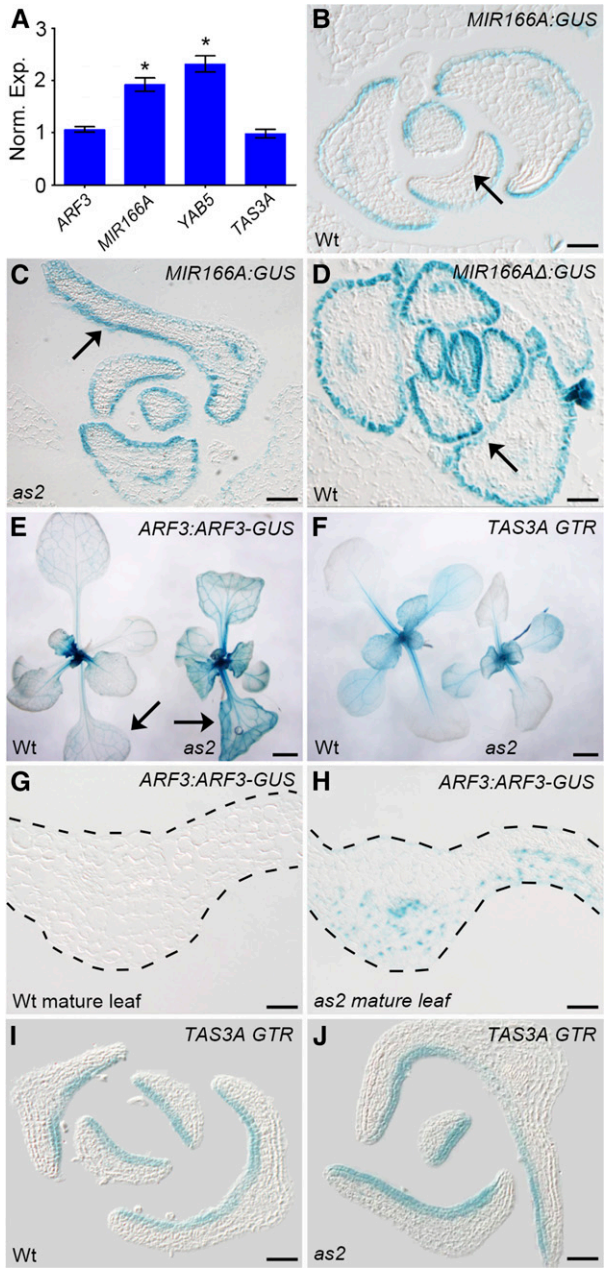

Figure 2. AS1-AS2 Employs Distinct Mechanisms to Regulate Its Polarity Targets.

(A) qRT-PCR analysis shows *MIR166A* and *YAB5* transcript levels are elevated in young leaves of *as2*, while *ARF3* and *TAS3A* levels remain unchanged. Expression values (means ± SE) normalized to the wild type were calculated based on at least three independent biological replicates (Student's *t* test; *$P < 0.05$). **(B)** to **(D)** *MIR166A:GUS* reporter activity is restricted to the abaxial epidermis of wild-type primordia **(B)** but is ectopically expressed in the adaxial epidermis (arrows) in *as2* **(C)** and in leaves of wild-type plants carrying a *MIR166AΔ:GUS* transgene with deleted AS1-AS2 binding sites **(D)**. **(E)** *ARF3:ARF3-GUS* reporter activity subsides to virtually undetectable levels in mature leaves of the wild type but remains high in mature leaves of *as2*. **(F)** By contrast, *TAS3A* gene trap activity is similar in wild-type and *as2* seedlings.

at *ARF3* but regulates its expression in a temporal rather than a spatial manner. Finally, in contrast to both *ARF3* and *MIR166A*, the spatial and temporal pattern of *TAS3A* expression is not obviously changed in *as2* (Figures 2F, 2I, and 2J), indicating a more complex relationship between AS1-AS2 and this direct target.

MIR166A and *YAB5* Accumulate H3K27me3 in an AS1-AS2-Dependent Manner

AS1-AS2 mediates the stable repression of *BP* and *KNAT2* in developing leaves via recruitment of Polycomb Repressive Complex2 (PRC2; Lodha et al., 2013). PRC2 deposits the H3K27me3-repressive chromatin mark at target loci to ensure their correct spatiotemporal expression, thus suggesting a potential mechanism by which AS1-AS2 might regulate *MIR166A*, *YAB5*, and *ARF3*. To investigate this possibility, we assessed the levels of H3K27me3 present at these genes in developing leaves of 12-d-old seedlings. Maximum enrichment of H3K27me3 at *BP* and *KNAT2* is seen between the proximal AS1-AS2 binding site and the transcription start site (Lodha et al., 2013). With this in mind, we analyzed levels of H3K27me3 at multiple sites in the promoters of *MIR166A*, *YAB5*, and *ARF3* (Figure 3A). As expected, chromatin at the known PRC2 target *SHOOTMERISTEMLESS* (*STM*) is highly enriched for H3K27me3 in comparison to the levels of this histone mark at the actively transcribed *ACTIN2* (*ACT2*) gene (Figure 3B; Lodha et al., 2013). A significant enrichment for H3K27me3 was also detected at all sites tested along the promoters of *MIR166A* and *YAB5* (Figure 3B). Levels of this silencing mark are lower at *MIR166A* than *STM*, perhaps reflecting the fact that *STM* activity is silenced in all cells of the primordium, whereas repression of *MIR166A* is polar and may be limited to the adaxial epidermis. This might also explain the H3K27me3 profile seen at *YAB5*, which remains active throughout the abaxial domain (Sarojam et al., 2010). Interestingly, no enrichment for H3K27me3 was detected at the *ARF3* promoter (Figure 3B). Analysis of additional regions upstream of the AS1-AS2 binding site and within the *ARF3* coding sequence itself also revealed no H3K27me3 deposition (Supplemental Figure 3). This finding is consistent with data from genome-wide H3K27me3 profiling studies (Zhang et al., 2007; Roudier et al., 2011) and supports the idea that distinct mechanisms are employed to repress expression of *MIR166A* and *YAB5*, versus *ARF3*.

To determine whether H3K27me3 at *MIR166A* and *YAB5* is deposited in an AS1-AS2-dependent manner, we compared the H3K27me3 profiles at these loci in the wild type and *as2*. Levels of H3K27me3 at *ACT2* and *STM* are not significantly changed in *as2* (Figure 3B); the latter being consistent with the fact that H3K27me3 deposition at *STM* occurs in an AS1-AS2-independent manner (Lodha et al., 2013). H3K27me3 levels along the promoters of both *MIR166A* and *YAB5*, however, are significantly reduced in *as2*

(G) and **(H)** Sections of mature wild-type leaves **(G)** show no *ARF3:ARF3-GUS* activity, whereas leaves of similarly staged *as2* plants **(H)** retain *ARF3:ARF3-GUS* signal in nuclei of abaxial cells. Black dashed lines flank the epidermal layers.

(I) and **(J)** Sections of wild-type **(I)** and *as2* **(J)** leaf primordia show equivalent *TAS3A* gene trap activity in the two adaxial-most cell layers. Bars = 50 μm in **(B)** to **(D)** and **(G)** to **(J)** and 0.5 cm in **(E)** and **(F)**.

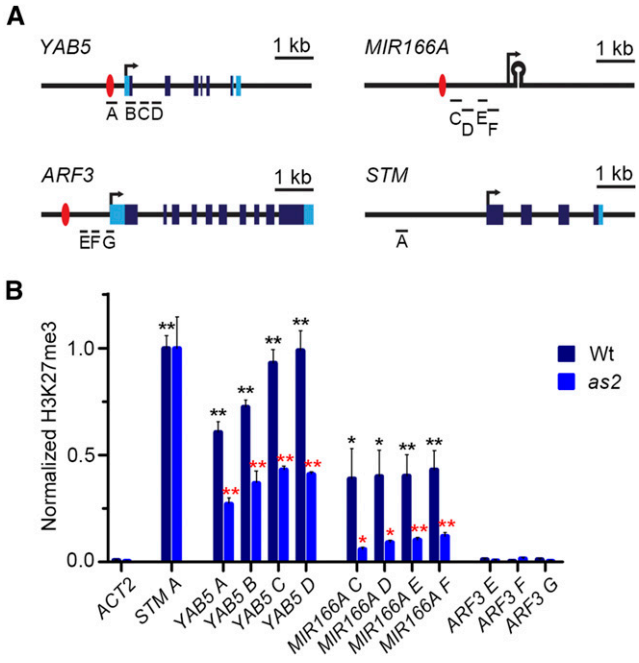

Figure 3. AS1-AS2 Employs PRC2-Dependent and -Independent Mechanisms to Regulate *YAB5*, *MIR166A*, and *ARF3* Expression.

(A) Schematic representations of *YAB5*, *MIR166A*, *ARF3*, and *STM* showing the positions of binding sites occupied by AS1-AS2 (red ovals), amplicons analyzed in ChIP (black bars), transcription start sites (arrow), untranslated regions (light-blue boxes), exons (dark-blue boxes), and the pre-miRNA of *MIR166A* (stem-loop). Letters below each amplicon correspond to primer pairs detailed in Supplemental Table 4.

(B) Levels of H3K27me3 at *YAB5*, *MIR166A*, and *STM* are enriched over the *ACT2* negative control (black asterisks), whereas levels of H3K27me3 at *ARF3* are indistinguishable from *ACT2*. H3K27me3 levels at *YAB5* and *MIR166A* are reduced in *as2* leaves relative to the wild type (red asterisks), whereas levels of H3K27me3 at the *ACT2* and *STM* controls remain unchanged. H3K27me3 values (means ± SE; $n \geq 3$) are normalized to H3 levels to correct for potential variations in nucleosome density and then further normalized to the *STM* positive control. Student's *t* test: *P < 0.05; **P < 0.01.

(Figure 3B). Given that AS1-AS2 physically interacts with multiple PRC2 components, these data present a model wherein AS1-AS2 guides PRC2 to the promoters of *MIR166A* and *YAB5* to catalyze the trimethylation of H3K27, much like the mechanism of repression of *BP* and *KNAT2* (Lodha et al., 2013). This silencing mechanism prevents the accumulation of *MIR166A* and *YAB5* on the adaxial side of developing primordia and identifies additional direct repressive interactions contributing to the mutual antagonism between adaxial and abaxial cell fates. Finally, while AS1-AS2 is required for the correct temporal repression of *ARF3*, this involves a distinct and PRC2-independent mechanism.

Convergent Regulation of *ARF3* by the AS and ta-siRNA Pathways Affects Leaf Architecture

To gain insight into the significance of *ARF3* regulation by AS1-AS2, we took into consideration that *ARF3* is also spatially regulated by tasiR-ARF (Chitwood et al., 2009). Loss of this convergent regulation may be required to unmask the contribution of AS1-AS2. Indeed, a strongly synergistic phenotype is observed when *as1* or *as2* alleles are introduced into plants mutant for ta-siRNA biogenesis (Garcia et al., 2006; Xu et al., 2006). However, the basis for this phenotype is not fully understood. Given the sensitivity of the leaf to ARF3 dosage (Fahlgren et al., 2006; Hunter et al., 2006), our data suggest expanded ARF3 activity not only spatially, but also temporally due to loss of AS1-AS2 activity, as a potential explanation. An alternative, non-mutually exclusive explanation derives from the mutual antagonism between adaxial and abaxial fates. Misregulation of abaxial determinants resulting from loss of AS1-AS2, in combination with ectopic expression of the abaxial determinants *ARF3* and *ARF4*, may confer enhanced abaxialized characteristics on double mutant leaves, resulting in adaxial-to-abaxial cell fate switches.

Therefore, to elucidate the consequences of AS1-AS2-mediated regulation of *ARF3*, we began to assay the nature of the synergistic interaction between the AS and ta-siRNA pathways by constructing a double mutant between the *as2-4* and *sgs3-1* null alleles. Compared with the wild type (Figures 4A, 4E, and 4I), *as2* seedlings are slightly dwarfed and develop rumpled, rounded leaves with a reduced petiole (Figures 4B, 4F, and 4J), whereas *sgs3* seedlings form elongated, more rectangular, and downward-curled leaves (Figures 4C, 4G, and 4K). *as2 sgs3* double mutants, like *as2*, have a reduced stature but produce smaller leaves with ridged blades that contain small outgrowths at their base (Figure 4D). These defects become progressively more severe, such that mature leaves of 27-d-old *as2 sgs3* plants appear highly dissected, with multiple outgrowths originating at the base of their blades (Figures 4H and 4L). These outgrowths are partially flattened and appear to arise at or near the margins of the main axis. Moreover, outgrowth formation in *as2 sgs3* leaves appears a reiterative process as, over time, secondary and tertiary outgrowths develop, always from proximal, marginal regions of established outgrowths (Figure 4L).

To understand the basis for the synergistic *as2 sgs3* phenotype, we first examined how regulation of *ARF3* dosage might contribute. Expression analysis showed that *ARF3* transcript levels in *sgs3* are elevated ~2-fold (Figure 4M). *ARF3* expression in *as2 sgs3* is increased even further, consistent with convergent regulation of *ARF3* by the AS and ta-siRNA pathways. However, tasiR-ARF also targets transcripts of *ARF2* and *ARF4* (Williams et al., 2005). To distinguish whether the synergistic phenotype of *as2 sgs3* is due to misregulation of multiple tasiR-ARF targets, or *ARF3* specifically, we further analyzed the expression levels of *ARF2* and *ARF4*. *ARF2* transcript levels in 12-d-old seedling leaves did not vary significantly for any genotype, while *ARF4* transcript levels are unchanged in *as2* and increased ~4-fold in *sgs3*. However, in contrast to *ARF3*, transcript levels for *ARF4* are not significantly different in developing *as2 sgs3* versus *sgs3* leaves (Figure 4M).

This finding correlates with the fact that only *ARF3* is a direct target of AS1-AS2 and suggests that misregulation of *ARF3* specifically contributes to the synergistic leaf phenotype of *as2 sgs3*. This possibility was verified genetically, as loss of *ARF3* function in *as2 sgs3* completely suppresses their dissection, giving rise to triple mutant plants that resemble *as2* in appearance

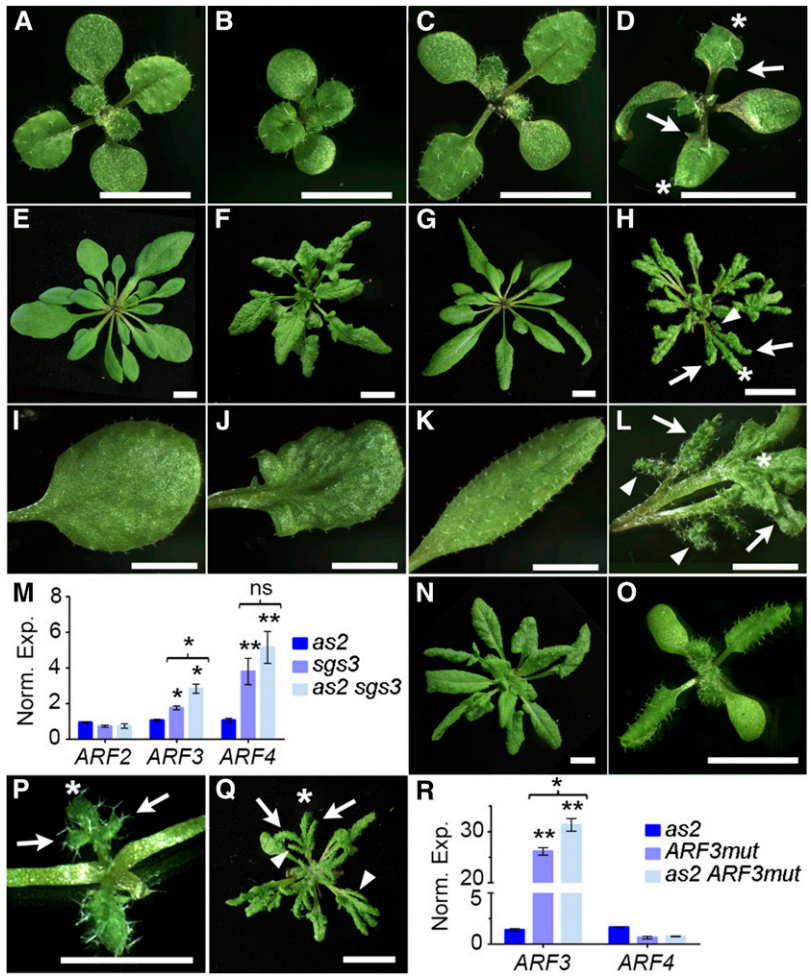

Figure 4. Compromising the AS and ta-siRNA Pathways Produces an *ARF3*-Dependent Synergistic Phenotype.

(A) to **(D)** Unlike 12-d-old wild-type **(A)**, *as2* **(B)**, and *sgs3* **(C)** plants, leaves of *as2 sgs3* **(D)** seedlings develop minor elaborations at their base (arrows).
(E) to **(H)** Twenty-seven-day-old wild-type **(E)**, *as2* **(F)**, *sgs3* **(G)**, and *as2 sgs3* **(H)** plants show this phenotype becomes progressively more severe.
(I) to **(L)** Compared with representative leaves of 27-d-old wild type **(I)**, *as2* **(J)**, and *sgs3* **(K)**, leaves of *as2 sgs3* **(L)** have a highly dissected morphology, developing secondary outgrowths (arrowheads) at the base of primary outgrowths (arrows).
(M) qRT-PCR shows transcript levels of *ARF2* are unchanged in young leaves of 12-d-old *as2*, *sgs3*, and *as2 sgs3* seedlings relative to the wild type, whereas *ARF3* and *ARF4* expression is increased specifically in *sgs3* and *as2 sgs3*. Note only *ARF3* transcript levels are increased further in *as2 sgs3* over *sgs3*.
(N) Twenty-seven-day-old *as2 sgs3 arf3* plants show complete suppression of the *as2 sgs3* dissected leaf phenotype.
(O) Twelve-day-old *ARF3:ARF3mut* seedlings show *ARF3* overexpression alone does not produce dissected leaves.
(P) and **(Q)** Twelve-day-old **(P)** and 27-d-old **(Q)** *as2 ARF3:ARF3mut* plants show this phenotype.
(R) qRT-PCR showing transcript levels of *ARF3* are dramatically elevated in young *ARF3:ARF3mut* and *as2 ARF3:ARF3mut* leaves but are unchanged in *as2*. Note that *ARF3* transcript levels are increased in *as2 ARF3:ARF3mut* over *ARF3:ARF3mut*. *ARF4* transcript levels, by contrast, do not differ between any genotype. Expression values (means ± SE) normalized to the wild type were calculated based on at least three independent biological replicates (Student's *t* test: ns, not significant; *P < 0.05; **P < 0.01).
Asterisks in **(D)**, **(H)**, **(L)**, **(P)**, and **(Q)** indicate primary leaf blade; arrows indicate primary outgrowth; arrowheads indicate secondary outgrowth. Bars = 1 cm.

(Figure 4N). By contrast, *as2 sgs3 arf4* triple mutants are indistinguishable from *as2 sgs3* double mutants (Supplemental Figure 4A). In addition, we crossed *as2* to a line expressing a tasiR-ARF-resistant form of *ARF3* under its native promoter (*ARF3:ARF3mut*; Fahlgren et al., 2006), which uncouples *ARF3* regulation from other aspects of the *sgs3* phenotype. *ARF3:ARF3mut* seedlings develop leaves that curl downward to a greater extent than *sgs3* (Figure 4O). Also, the phenotype of *as2 ARF3:ARF3mut* mutants is initially more severe than that of *as2 sgs3*, in that the degree of leaf dissection in *as2 ARF3:ARF3mut* seedlings is increased compared with *as2 sgs3* (Figures 4D and 4P; Supplemental Figures 4B and 4C). However, 27-d-old *as2 ARF3:ARF3mut* and *as2 sgs3* plants are largely indistinguishable (Figures 4H and 4Q). As expected, *ARF4* transcript levels are unaffected in both *ARF3:ARF3mut* and *as2 ARF3:ARF3mut* seedlings (Figure 4R). *ARF3* transcripts, on the other hand, accumulate to significantly higher levels in

ARF3:ARF3mut seedlings than in *sgs3* (Figures 4M and 4R), and these levels are further increased in *as2 ARF3:ARF3mut* double mutants.

These data highlight the importance of *ARF3* regulation by AS1-AS2 to leaf development. While loss of ta-siRNA regulation conditions misexpression of both *ARF3* and *ARF4*, only prolonged ectopic expression of the AS1-AS2 target *ARF3* is required for the altered leaf morphology seen in AS and ta-siRNA pathway double mutants. Supporting this, *ARF3* is correctly positioned to regulate the formation of ectopic outgrowths, as the *ARF3:ARF3-GUS* reporter marks their sites of initiation in *as2 sgs3* (Supplemental Figures 4D and 4E). However, ectopic *ARF3* expression alone is not sufficient to condition the *as2 sgs3* phenotype, as leaves of *ARF3:ARF3mut* do not show this defect (Figure 4O; Fahlgren et al., 2006). Prolonged ARF3 activity is likewise insufficient, as *as2* mutants, or plants constitutively expressing *ARF3mut*, also fail to develop this phenotype (Figure 4F; Hunter et al., 2006). This indicates that another aspect of the *as2* phenotype converges with altered *ARF3* expression to regulate leaf architecture.

Contributions of *ARF3* to Leaf Development beyond Adaxial-Abaxial Patterning

Indeed, an alternative, or complementary, hypothesis to explain the synergistic phenotype of leaves compromised for both the AS and ta-siRNA pathways is a further increase in abaxial identity. To evaluate this hypothesis, we compared the expression level of central adaxial and abaxial polarity determinants in developing wild-type, *as2*, *sgs3*, and *as2 sgs3* leaves (Figures 5A and 5B). Beyond the direct targets *MIR166A* and *YAB5*, none of the genes tested show a significant change in expression in *as2* versus wild-type seedlings. Likewise, only transcript levels for the direct ta-siRNA targets *ARF3* and *ARF4* are significantly changed in *sgs3*. However, in *as2 sgs3*, transcript levels for *YAB5* and *ARF3* are increased above the levels seen in *as2* and *sgs3*. In addition, expression of the abaxial determinants *FIL* and *KAN1* is also elevated, suggesting *as2 sgs3* leaves are abaxialized to a greater extent than either single mutant. Consistent with this finding, and the mutually antagonistic relationship between adaxial and abaxial cell fates, a concomitant reduction in expression of the adaxial determinants *AGO7*, *TAS3A*, *PHB*, *REV*, and *AS2* is detected in *as2 sgs3*. Of particular note, the transcript levels of *TAS3A* and *AGO7* are dramatically reduced specifically in the *as2 sgs3* double mutant (Figure 5B), hinting at a more complex relationship between *ARF3* and the ta-siRNA pathway that patterns its activity.

A greater degree of abaxialization of developing *as2 sgs3* leaves was also evident from analysis of *FIL* and *TAS3A* reporters. In agreement with the described *FIL* mRNA expression pattern (Siegfried et al., 1999), the *FIL:GUS* reporter accumulates on the abaxial side of wild-type primordia (Figure 5C). This expression domain is unchanged in *as2* and *sgs3* (Figures 5D and 5E), but *FIL* expression extends into the adaxial domain of *as2 sgs3* primordia, consistent with a switch from adaxial to abaxial identity in these cells (Figure 5F). Moreover, whereas the *TAS3A* gene trap is adaxially expressed in wild-type, *as2*, and *sgs3* leaf primordia, its activity is severely reduced in *as2 sgs3* (Figures 5G to 5J). Extremely weak *TAS3A* gene trap activity specifically in *as2 sgs3* mutants is consistent with the dramatic reduction of *TAS3A* transcript levels in this genotype (Figure 5B) and demonstrates that repression of this adaxial determinant occurs at the transcriptional level. This finding is particularly intriguing given that *TAS3A* is a direct target of AS1-AS2 and suggests that the contribution of these DNA binding factors to *TAS3A* regulation is only apparent when *ARF3* and/or *ARF4* is ectopically expressed.

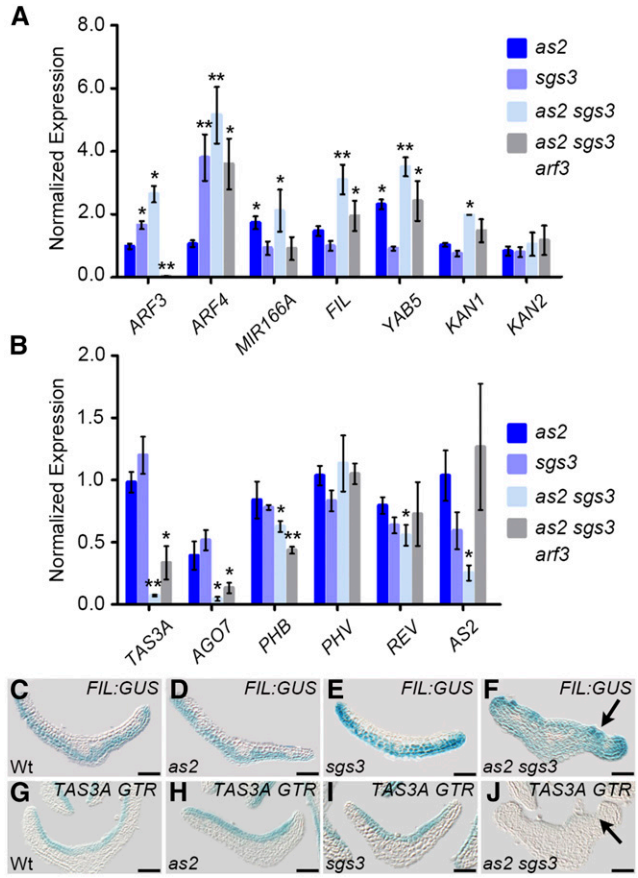

Figure 5. Both *as2 sgs3* and *as2 sgs3 arf3* Leaves Are Partially Abaxialized.

(A) qRT-PCR on young leaves of 12-d-old seedlings reveals transcript levels of many key abaxial determinants are synergistically elevated in *as2 sgs3* over *as2* and *sgs3* single mutants. This elevation is suppressed for some, but not all, in *as2 sgs3 arf3*.

(B) Conversely, transcript levels of many adaxial determinants are synergistically reduced in 12-d-old *as2 sgs3* leaves relative to *as2* and *sgs3* and are partially returned in *as2 sgs3 arf3*. Note the dramatic reductions in *TAS3A* and *AGO7* transcript levels specifically in *as2 sgs3*, which remain low in *as2 sgs3 arf3*. Expression values (means ± SE) normalized to the wild type were calculated based on at least three independent biological replicates (Student's *t* test: *P < 0.05; **P < 0.01).

(C) to **(F)** *FIL:GUS* reporter activity is restricted to the abaxial domain of wild-type **(C)**, *as2* **(D)**, and *sgs3* **(E)** primordia but is ectopically expressed in the adaxial domain (arrow) of young *as2 sgs3* leaves **(F)**.

(G) to **(J)** *TAS3A* gene trap activity in the two adaxial-most cell layers of wild-type **(G)**, *as2* **(H)**, and *sgs3* **(I)** primordia is barely detectable (arrow) in *as2 sgs3* **(J)**. Note: Images in **(G)** and **(H)** are taken from Figures 2J and 2K, respectively. Bars = 50 μm in **(C)** to **(J)**.

This prospect is in line with the earlier notion that AS1-AS2-mediated regulation of *TAS3A* employs a mechanism distinct from that utilized to regulate *MIR166A*, *YAB5*, and *ARF3*.

These data show that *as2 sgs3* mutant leaves are molecularly abaxialized to a greater extent than leaves of either *as2* or *sgs3*. To investigate whether this synergistic effect on adaxial-abaxial polarity is primarily responsible for the apparent dissection of *as2 sgs3* leaves, we examined expression of adaxial and abaxial determinants also in *as2 sgs3 arf3* triple mutants that show a complete suppression of this defect (Figure 4N). Transcripts for select polarity determinants, including *KAN1*, *REV*, and *AS2*, no longer show a significant difference in expression in developing *as2 sgs3 arf3* leaves compared with the wild type (Figures 5A and 5B). However, transcript levels of the abaxial determinants *FIL*, *YAB5*, and *ARF4*, and the adaxial determinants *AGO7*, *TAS3A*, and *PHB*, remain significantly changed (Figures 5A and 5B), indicating that *as2 sgs3 arf3* triple mutants remain partially abaxialized at the molecular level, despite a complete suppression of the deep dissection of their leaves. This finding is consistent with the fact that *ARF4*, like *ARF3*, promotes abaxial identity (Pekker et al., 2005). It further shows that misexpression of *ARF4* in an *as2* background is sufficient to repress *TAS3A* and *AGO7* expression, though not to the same extent as when *ARF3* is simultaneously misexpressed. However, the fact that *as2 sgs3 arf3* leaves remain partially abaxialized implies that a synergistic effect of mutations in both the AS and ta-siRNA pathways on adaxial-abaxial polarity is insufficient to condition the phenotype seen in *as2 sgs3* and *as2 ARF3:ARF3mut* leaves. These observations point to a role for AS1-AS2 in the regulation of leaf dissection that is mediated via its direct target *ARF3* but is distinct from its contribution to adaxial-abaxial patterning. This regulation further identifies a function for ARF3 that is not shared by its close homolog ARF4.

Outgrowths on *as2 sgs3* Leaves are Modified Serrations with Proximodistal Polarity

The notion that regulation of *ARF3* by AS1-AS2, as well as tasiR-ARF, affects leaf morphology in a manner distinct from their role in adaxial-abaxial patterning is supported by the appearance of the *as2 sgs3* outgrowths themselves. While mutants with defects in adaxial-abaxial polarity frequently develop ectopic outgrowths, these are new mediolateral axes that arise from ectopic adaxial-abaxial boundaries on the upper or lower surface of the leaf blade and extend minimally (Waites and Hudson, 1995; Eshed et al., 2001; Pekker et al., 2005). Outgrowths on *as2 sgs3* leaves, by contrast, appear to arise at or near the margins, are highly elaborated, and form in a reiterative fashion (Figure 4L).

To further address the nature of these outgrowths, we analyzed their morphogenesis using scanning electron microscopy. Young leaves of 12-d-old *as2 sgs3* seedlings show elaborations at the proximal margins of the blade that are not present in the wild type, *as2*, or *sgs3* (Figures 6A to 6D). Analysis of earlier primordial stages suggests these marginal outgrowths initiate as large dome-shaped structures at sites normally occupied by serrations, which by contrast, emerge as relatively flat and pointed structures (Figures 6G and 6H). Moreover, unlike the simple protrusions seen in adaxial-abaxial polarity mutants, these *as2 sgs3* outgrowths eventually develop into structures with a well-defined proximodistal axis.

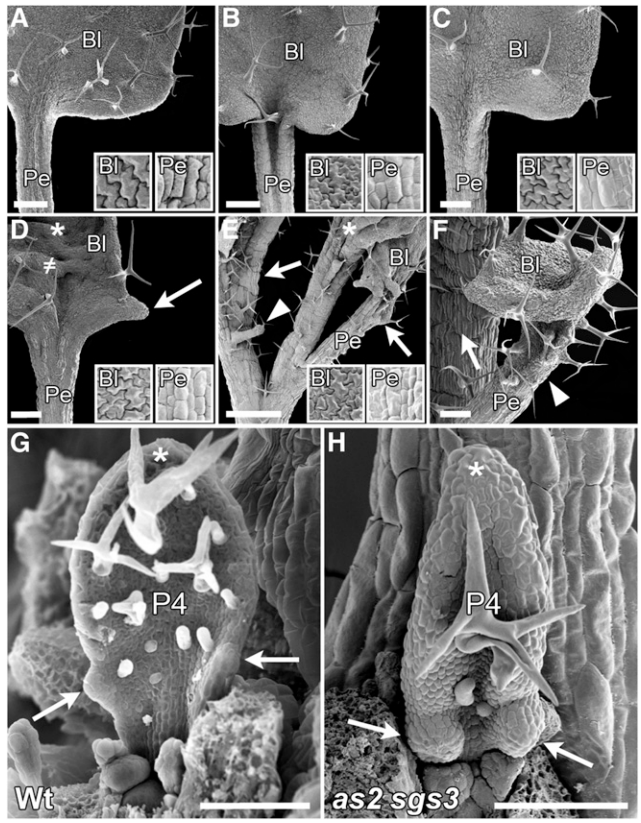

Figure 6. *as2 sgs3* Outgrowths Originate at Proximal Blade Margins and Possess a Distinct Proximodistal Axis.

(A) to **(D)** Unlike the wild type **(A)**, *as2* **(B)**, and *sgs3* **(C)**, 12-d-old *as2 sgs3* seedling leaves **(D)** develop minor elaborations from the proximal blade margin (arrow) and ridges (≠) on the upper surface of the primary blade (asterisk). Leaves of all genotypes possess proximodistal polarity, as evidenced by discrete blade (Bl) and petiole (Pe) cell morphologies (insets). **(E)** and **(F)** A representative leaf from a 37-d-old *as2 sgs3* plant shows primary outgrowths (arrows) develop a well-defined proximodistal axis **(E)**, as do the secondary outgrowths (arrowheads) that arise at their base **(F)**. **(G)** and **(H)** Scanning electron micrograph of plastochron 4 (P4) wild-type **(G)** and *as2 sgs3* (**H**) leaf primordia shows serrations (arrows in **[G]**) and primary outgrowths (arrows in **[H]**) arise at equivalent marginal positions but have different morphologies. Note, unlike wild-type serrations, *as2 sgs3* outgrowths are dome-shaped.
Asterisks indicate primary leaf blade; arrows indicate primary outgrowth; arrowheads indicate secondary outgrowth; ≠, adaxial ridges. Bars = 250 μm in **(A)** to **(D)** and **(F)**, 1 mm in **(E)**, and 100 μm in **(G)** and **(H)**.

Epidermal cells of the petiole and blade of Arabidopsis leaves can be easily distinguished, as petiole cells have a rectangular morphology, oriented parallel to the proximodistal axis of the leaf, whereas blade cells are irregularly shaped with interdigitated lobes (Figure 6, insets). Despite their altered morphology, *as2*, *sgs3*, and *as2 sgs3* leaves develop clearly defined petiole and blade regions (Figures 6B to 6D). Importantly, this morphology is also evident in *as2 sgs3* outgrowths, as cells in the flattened distal area show blade characteristics while cells in the proximal regions resemble petiole cells (Figure 6E). Even secondary outgrowths on *as2 sgs3* leaves show

distinct petiole and blade morphologies (Figure 6F). Consistent with the enhanced abaxialized nature of this genotype, blades of individual outgrowths on *as2 sgs3* leaves do show characteristics of adaxial-abaxial polarity mutants that are not obvious in either *as2* or *sgs3*. These develop a rough upper surface with ridged blade-like outgrowths associated with reduced adaxial identity (Figures 6D and 6E), and occasionally individual outgrowths take on a trumpet-shaped morphology (Figure 6F). However, both expression and morphogenetic analyses indicate that the primary basis for the marginal proximodistal outgrowths on *as2 sgs3* leaves is not a defect in adaxial-abaxial patterning.

The AS and ta-siRNA Pathways Converge to Suppress Leaf Complexity

As defective adaxial-abaxial polarity is insufficient to explain the marginal outgrowths of *as2 sgs3*, what then might underlie their biogenesis, and how might AS1-AS2 regulation of *ARF3* contribute? Considering *ARF3* modulates the auxin response, and auxin maxima are known to drive outgrowth in a variety of developmental contexts, including the formation of leaves from the meristem, and leaflets or serrations from the leaf margin (Benková et al., 2003; Reinhardt et al., 2003; Heisler et al., 2005; Koenig and Sinha, 2010; Bilsborough et al., 2011), auxin signaling emerges as a plausible contributor. We therefore examined the pattern of PIN-FORMED1 (PIN1) localization during primordium development using the *PIN1:PIN1-GFP* reporter (Benková et al., 2003). Within the sixth leaf of 10- and 12-d-old wild-type, *as2*, and *sgs3* seedlings, PIN1-GFP is expressed at sites of incipient serrations (Supplemental Figures 5A and 6). Consistent with previous reports (Koenig and Sinha, 2010; Bilsborough et al., 2011), PIN1-GFP localization within the epidermis of serrations is polarized, predicting auxin is transported toward a convergence point at the serration tip. As normal leaves mature, PIN1-GFP expression dissipates and is undetectable in the same leaf of 16-d-old seedlings (Figure 7A; Supplemental Figure 6). The PIN1-GFP dynamics in *sgs3* are indistinguishable from the wild type (Figure 7C; Supplemental Figure 6). In *as2*, however, PIN1-GFP activity persists and marks new serrations at the base of the sixth leaf even in 16- and 18-d-old plants (Figure 7B; Supplemental Figure 6).

Prolonged PIN1 activity is even more pronounced in *as2 sgs3* leaves, where PIN1-GFP is detectable 27 d postgermination (Supplemental Figure 6). At 16 d, primary outgrowths on the sixth leaf of *as2 sgs3* are significantly more elaborated than the serrations that occupy these sites in other genotypes and acquire discrete PIN1-GFP foci at their base (Figure 7D). The pattern of PIN1-GFP polarization at these sites is reminiscent of that seen in young leaf primordia (Supplemental Figure 5B), consistent with these primary outgrowths possessing a functional proximodistal axis (Figures 6E and 6F). Furthermore, these foci mark the sites of secondary outgrowths, which, upon elaboration, also generate new PIN1-GFP foci at their base (Supplemental Figure 5C). The spatial pattern and prolonged expression of PIN1-GFP thus correlates with the reiterative nature of outgrowths on leaves perturbed in both the AS and ta-siRNA pathways, predicting a role for polar auxin transport in their formation. To directly test this prediction, the severe *as2 ARF3:ARF3mut* double mutant was grown on media containing the auxin transport inhibitor 1-*N*-naphthylphthalamic acid (NPA). Wild-type, *as2*, and *ARF3:ARF3mut* seedlings show minor changes in leaf shape in response to NPA treatment (Figures 7E to 7G and 7I to 7K). Formation of elaborated outgrowths on *as2 ARF3:ARF3mut* leaves, by contrast, is completely suppressed (Figures 7H and 7L), indicating that PIN1-derived auxin transport is required for their formation.

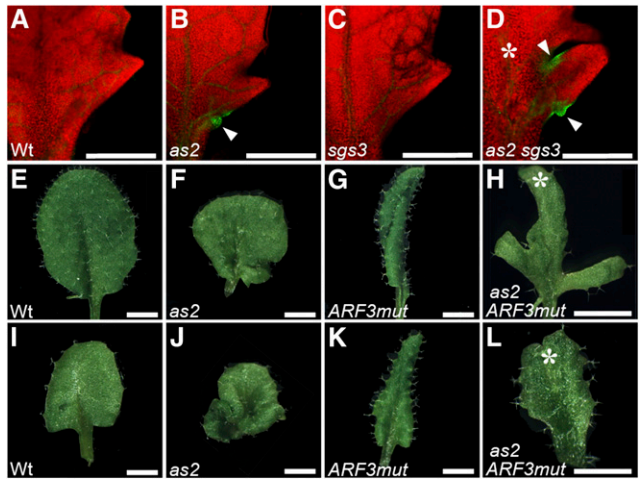

Figure 7. *as2 sgs3* Outgrowths Are Presaged by PIN1-GFP Foci and Their Biogenesis Requires Functional Polar Auxin Transport.

(A) to **(D)** Confocal imaging of 16-d-old *PIN1:PIN1-GFP* seedlings shows that, unlike the wild type **(A)** and *sgs3* **(C)**, the fifth leaves of *as2* **(B)** and *as2 sgs3* **(D)** seedlings retain foci of PIN1-GFP activity at their margin. In *as2 sgs3*, this PIN1-GFP signal correlates with formation of secondary outgrowths (arrowheads) from primary outgrowths (arrow).
(E) to **(L)** Seedling leaves grown in the absence (**[E]** to **[H]**) or presence (**[I]** to **[L]**) of 5 μM NPA reveal that wild-type (**[E]** and **[I]**), *as2* (**[F]** and **[J]**), and *ARF3:ARF3mut* (**[G]** and **[K]**) leaf morphology is largely unperturbed by treatment with NPA, while leaves of *as2 ARF3:ARF3mut* (**[H]** and **[L]**) show a complete suppression of their dissected leaf phenotype.
Asterisks indicate primary leaf blade; arrows indicate primary outgrowth; arrowheads indicate secondary outgrowth. Bars = 400 μm in **(A)** to **(D)** and 1 mm in **(E)** to **(L)**.

The fact that the outgrowths in *as2 sgs3* are elaborated serrations with a well-defined proximal-distal axis suggests parallels between these outgrowths and leaflets of compound-leafed species. Formation of leaflets in most compound-leafed species is also associated with expression of indeterminacy-promoting KNOX genes in leaf primordia (Bharathan et al., 2002; Hay and Tsiantis, 2006; Barkoulas et al., 2008). In this regard, it is interesting that ectopic ARF3 activity alone is insufficient to drive the formation of proximodistal outgrowths and that another aspect of the *as2* phenotype is required. AS1-AS2 mediates the repression of both *BP* and *KNAT2* in developing leaves (Guo et al., 2008), though only the levels of *BP* change dramatically in *as2* (Ori et al., 2000; Semiarti et al., 2001; Lodha et al., 2013). Indeed, while unaffected in *sgs3*, *BP* is strongly misexpressed in *as2 sgs3* and *as2 sgs3 arf3* leaves (Supplemental Figure 5D).

Taken together, these data reveal that the direct regulation of *ARF3* by AS1-AS2 contributes in a surprisingly multifaceted way to leaf development. The AS pathway converges with the ta-siRNA

pathway to limit *ARF3* expression both spatially and temporally. Loss of this convergent regulation results in an enhanced abaxialized phenotype, characterized by a dramatic reduction in *TAS3A* transcription, as well as an *ARF3*-dependent increase in leaf complexity. These phenotypes show that the shared repression of *ARF3* by the AS and ta-siRNA pathways intersects with additional AS1-AS2 targets to affect multiple nodes in leaf development, thereby keeping the Arabidopsis leaf both flat and simple.

DISCUSSION

AS1-AS2 Uses Distinct Mechanisms to Regulate Its Polarity Targets

The control of adaxial-abaxial leaf polarity must be extremely robust. In addition to differentiating distinct cell types on the leaf's top and bottom faces, the boundary between adaxial and abaxial fates provides positional information that drives the flattened outgrowth of the leaf blade (Waites and Hudson, 1995; Nakata et al., 2012). Flatness is not a default state but results from precise coordination of cell division and differentiation, such that even slight perturbations in adaxial-abaxial polarity lead to leaf curling and other morphological changes. Formation of the flat leaf thus poses an interesting mechanistic challenge, namely, how to create a stable boundary throughout the plane of a long and wide, yet shallow, structure. The clean separation of adaxial and abaxial fates, at both the cell and the domain level, relies on positive and negative feedback regulation between polarity determinants that reinforce initial cell fate decisions (Husbands et al., 2009). However, few of these regulatory interactions are understood at the mechanistic level. In particular, the molecular relationships between the conserved transcription factors at the core of the adaxial-abaxial polarity network remain poorly understood.

Here, we investigated the contribution of AS1-AS2 to adaxial-abaxial patterning and show that *MIR166A*, *YAB5*, *ARF3*, and *TAS3A* are direct targets for this adaxial determinant. Interestingly, AS1-AS2 makes discrete contributions to the regulation of these targets and employs distinct molecular mechanisms to regulate their expression. At *MIR166A*, AS1-AS2 prevents transcription in the adaxial epidermal layer and is thus required for the correct spatial regulation of this microRNA. AS1-AS2 may also help define the spatial expression domain of *YAB5*. Like *MIR166A*, *YAB5* expression is normally restricted to the abaxial side of developing leaves (Sarojam et al., 2010) and increases in *as2* mutants. Repression of both *MIR166A* and *YAB5* by AS1-AS2 involves a PRC2-dependent mechanism, perhaps reminiscent of the AS1-AS2-based repression of the KNOX targets *BP* and *KNAT2* (Lodha et al., 2013).

The spatial restriction of abaxial factors like *MIR166A*, and possibly *YAB5*, by the adaxial factor AS1-AS2 reveals new direct interactions within the polarity network that are in line with the mutually exclusive nature of these two cell fates. The effect of AS1-AS2 on *ARF3* regulation, on the other hand, appears to be temporal in nature, ensuring abaxially localized ARF3 subsides as the leaf matures. This raises the question of how adaxial determinants might directly repress a target in the complementary abaxial domain. One explanation follows from the dynamic expression pattern of *AS2*, which overlaps with *AS1* throughout initiating leaf primordia before being localized to the adaxial side (Iwakawa et al., 2007). This initially uniform accumulation, which nucleates epigenetic change at *BP* and *KNAT2* (Lodha et al., 2013), may similarly initiate epigenetic change at *ARF3*, although not via PRC2. Given the duration of *ARF3* expression, this repression would also have to proceed more slowly, perhaps employing a mechanism similar to the H3K9me2-depositing complex *GIANT KILLER*, which gradually silences *ARF3* in the inflorescence (Ng et al., 2009). Alternatively, AS1-AS2 is known to form complexes with several distinct protein partners, including other chromatin regulators, presenting several potential mechanisms via which to mediate the temporal regulation of *ARF3* (Yang et al., 2008; Luo et al., 2012; Rast and Simon, 2012).

Interestingly, AS1-AS2 also binds the promoter of *TAS3A*, an adaxial determinant. The expression domain of *TAS3A* mirrors that of *AS2*, and its transcriptional output remains unchanged in *as2* mutants. These data indicate that AS1-AS2 does not always function in a repressor complex and has varied effects on target transcription, a behavior shared by many transcription factors (reviewed in Biggin, 2011). Moreover, meta-analyses of transcription factor occupancy across the genome reveal that these proteins are often present at considerably more loci than they are known to regulate. In particular, the many weak, low-occupancy interactions that transcription factors make may not directly regulate transcription at nearby genes. Rather, such interactions are thought to affect transcription indirectly by promoting or inhibiting the recruitment of other transcription factors (Biggin, 2011).

Our findings suggest that AS1-AS2 may, in fact, contribute to the regulation of *TAS3A* via this latter mechanism. Transcript levels of *TAS3A* are reduced far beyond that of other adaxial determinants when *ARF3* or *ARF4* are adaxially expressed in an *as2* background. Like other ARF proteins, ARF3 and ARF4 bind auxin response elements, but repress rather than activate target transcription (Tiwari et al., 2003). Interestingly, the *TAS3A* promoter contains a canonical auxin response and enhancer element pair immediately flanked by the AS1-AS2 binding sites, presenting the possibility that AS1-AS2 uses a "protective mechanism" to prevent downregulation of *TAS3A* on the adaxial side via stearic hindrance of ARF binding to its promoter. In this scenario, only in an *as1* or *as2* background would ARF3 and ARF4 be able to bind its *cis*-elements and downregulate *TAS3A* on the adaxial side. Additionally, repression of *TAS3A* may result from cooperativity between ARF3/ARF4 and factors that are misexpressed only in *as2*. One such candidate is KAN1, which physically interacts with ARF3 (Kelley et al., 2012), and whose expression extends into the adaxial side of *as2* leaves (Wu et al., 2008). The fact that *TAS3A* expression persists in *as2* seems to favor the requirement of a cofactor during the ARF3/ARF4-mediated repression of *TAS3A*. This hypothesis also nicely explains why ubiquitous ARF3 expression is insufficient to trigger adaxial-to-abaxial cell fate switches on its own (Fahlgren et al., 2006; Hunter et al., 2006).

Thus, AS1-AS2 employs at least three distinct mechanisms to regulate its polarity targets: (1) a Polycomb-mediated mechanism in the spatial regulation of targets such as *MIR166A* and *YAB5*; (2) a non-Polycomb-mediated, but still potentially epigenetic, mechanism in the temporal repression of *ARF3*; and (3) a nonrepressive, and possibly protective, mode of regulation at *TAS3A*.

Further Roles for AS1-AS2 in Adaxial-Abaxial Patterning

How might these molecular interactions contribute to adaxial-abaxial patterning? Adaxial-abaxial polarity is already evident within the incipient primordium (or P0), during which key polarity determinants, such as the HD-ZIPIII transcription factors, show a polar localization (Juarez et al., 2004; Heisler et al., 2005). The outcomes of surgical experiments, however, predict a brief developmental window during which organ polarity is resolved (Sussex, 1951; Reinhardt et al., 2005). Once in place, this polar axis is then stably maintained until the leaf differentiates. Given the severity of mutants expressing a miR166-resistant HD-ZIPIII allele (McConnell et al., 2001), spatial regulation of HD-ZIPIII expression, as patterned by polarized miR166 activity, forms a critical component in the establishment of adaxial-abaxial polarity. The detection of *MIR166A:GUS* reporter activity at the earliest stages of leaf development (Supplemental Figure 2A), and the strongly adaxialized phenotype of plants ubiquitously expressing *AS2* (Lin et al., 2003), support a prominent role for this *MIR166* member in particular early in adaxial-abaxial patterning.

This indicates that *MIR166A* expression must somehow be polarized at leaf initiation, which raises an intriguing question: How could AS1-AS2 silence *MIR166A* specifically on the adaxial side while silencing KNOX targets uniformly across the primordium? This might imply the existence of additional polarized cofactors that promote silencing of *MIR166A* in adaxial cells or block its repression in abaxial cells. However, the adaxialized phenotype resulting from ectopic expression of *AS2* (Lin et al., 2003) demonstrates AS1-AS2 can function on both sides of developing primordia. Rather, the polarized repression of *MIR166A* may reflect inherent properties of chromatin dynamics.

The switch from active to repressive chromatin is thought to involve a bistable epigenetic state that is resolved once nucleation of PRC2 elevates H3K27me3 levels beyond a certain threshold, triggering the spread of this repressive mark across the locus (Angel et al., 2011). *AS1* and *AS2* are only briefly coexpressed throughout a new primordium before *AS2* expression is restricted to the adaxial side (Iwakawa et al., 2007). Thus, the polarized repression of *MIR166A* may reflect a requirement for persistent AS1-AS2 occupancy before H3K27me3 levels can surpass the threshold needed to trigger stable silencing. This hypothesis can explain why prolonged misexpression of *AS2* across developing primordia conditions a strongly adaxialized phenotype (Lin et al., 2003). That repression of *BP* and *KNAT2* is nonpolar, despite employing a similar regulatory mechanism, might suggest that the establishment of a stable state occurs more rapidly at these loci. In this regard, it is intriguing that both KNOX promoters contain two AS1-AS2 binding sites that act cooperatively to mediate this silencing (Guo et al., 2008), whereas AS1-AS2 occupies a single site at *MIR166A*. This paradigm also fits the regulatory dynamics of *YAB5*, which is similarly bound by AS1-AS2 at a single site and remains active in abaxial cells (Sarojam et al., 2010).

A key question then is how the activity of *AS2* becomes polarized in developing primordia. KAN proteins directly repress *AS2* expression (Wu et al., 2008), making them likely candidates to set up this polarized activity. Indeed, KAN dynamics appear complementary to *AS2*, with transcripts accumulating on the abaxial side of developing leaves (Kerstetter et al., 2001; Wu et al., 2008). Furthermore, KAN proteins are excluded from the P0, which is defined by high levels of the KAN1-repressed target PIN1, and instead accumulate in a ring below initiating organs (Merelo et al., 2013; Yadav et al., 2014).

Taken together, these observations suggest a model that incorporates expression dynamics of key adaxial and abaxial determinants to explain the establishment and resolution of polarity (Figure 8). The exclusion of KAN proteins from the P0 allows the nonpolar accumulation of AS1-AS2 and the initial nucleation of PRC2-mediated H3K27me3 at the promoter of *MIR166A* on both sides of the primordium. As the primordium develops, KAN expression extends into its abaxial side (Yadav et al., 2014), directly repressing *AS2* expression and restricting further deposition of H3K27me3 at *MIR166A* solely to the adaxial side. This polarizes the production of mature miR166 and consequently limits HD-ZIPIII accumulation to the adaxial side.

However, this model implies that *MIR166A* itself is not expressed in the P0, raising the question of where miR166, which patterns HD-ZIPIII activity in the incipient primordium, originates. One possibility is that miR166 originates in the KAN-expressing region below the incipient leaf, an idea first posited in maize (*Zea mays*; Juarez et al., 2004). Indeed, *MIR166A* is a direct target of KAN1 and is not downregulated by this repressor protein (Merelo et al., 2013). Mobility of mature miR166 from a primordium-independent source could provide the positional information required to pattern HD-ZIPIII activity until the mechanisms within the primordium itself resolve to maintain adaxial-abaxial polarity. This can also explain why loss of AS1-AS2-directed silencing of *MIR166A* within the primordium does not condition a strong

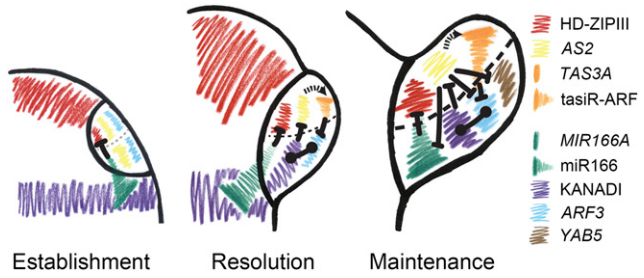

Figure 8. Model Describing the Establishment, Resolution, and Maintenance of Adaxial-Abaxial Polarity.

The incipient primordium (left panel) is polarized by a primordium-independent source of miR166, which moves from the internode below into the P0 and limits HD-ZIPIII activity to the adaxial side. This initial polarity is resolved from an externally to an internally patterned process as the primordium develops and KAN proteins become active on the abaxial side. KAN proteins, possibly in complex with ARF3, restrict *AS2* expression and thereby AS1-AS2 activity to the adaxial side, polarizing its downstream effects (middle panel). Once resolved, polarity is then stably maintained throughout primordium development through opposing miR166 and tasiR-ARF gradients acting on the domain level and mutually antagonistic interactions and positive feedback regulation of polarity determinants at the cellular level (right panel). More detailed descriptions of these interactions are presented in the text. T-bars denote direct repressive interactions, whereas the dotted arrow denotes a nonrepressive, possibly protective, interaction. The dumbbell denotes protein-protein interaction.

HD-ZIPIII loss-of-function phenotype, as AS1-AS2 is not predicted to act outside the incipient leaf.

The model thus predicts that sequential polarization of polarity factors is critical to adaxial-abaxial patterning. This process is established by polarity determinants originating from outside the incipient leaf, but as the primordium develops, polar expression patterns of adaxial and abaxial determinants within the primordium itself resolve. These are then stably maintained throughout leaf development by further positive and negative feedback between the polarity determinants (Figure 8).

A protective mechanism of action for AS1-AS2 at *TAS3A* (see above) is also in line with our current understanding of the spatiotemporal dynamics of the polarity network. ARF3 is present throughout the incipient leaf, as tasiR-ARF biogenesis is delayed until later in primordium development (Chitwood et al., 2009). The exclusion of KAN activity from the P0, however, predicts ARF3-directed *TAS3A* repression is blocked at this developmental stage, as AS1-AS2 is active throughout. Subsequent extension of KAN activity into the primordium would then limit the effect of AS1-AS2 on *TAS3A* to the adaxial side and permit ARF3/ARF4-mediated repression, possibly aided by a cofactor, on the abaxial side (Figure 8). This creates a feedback loop wherein the targets of tasiR-ARF polarize its biogenesis, thereby reinforcing the small RNA gradient that patterns them.

Thus, the dynamic localization of AS1-AS2 contributes to the polarization of *MIR166A* as well as the *TAS3A*-derived tasiR-ARF gradient. Intercellular movement of these small RNAs provides positional information to separate adaxial and abaxial fates at the domain level, by polarizing HD-ZIPIII and *ARF3*/*ARF4* accumulation, respectively. As such, AS1-AS2 stabilizes the separation of the adaxial and abaxial domains as polarity in the developing primordium transitions from an externally to an internally patterned process (Figure 8). In addition, AS1-AS2 reinforces adaxial identity at the cellular level through direct, Polycomb-mediated repression of the abaxial determinant *YAB5*. However, as YABBY genes display considerable variability in expression patterns across species (Husbands et al., 2009), the regulatory relationships between them and orthologous AS1-AS2 complexes remain an open and intriguing question. Taken together, our data reveal how the versatile regulatory properties of AS1-AS2 impact the robust placement of the adaxial-abaxial boundary, contributing to the production of a flat leaf.

The AS and ta-siRNA Pathways Intersect at Multiple Developmental Nodes

Our analyses further show that AS1-AS2 intersects with the ta-siRNA pathway to regulate *ARF3*, contributing to leaf development in a surprisingly multifaceted way. Loss of both pathways results in enhanced abaxialized defects, which are not simply explained by the synergistic misexpression of their shared target *ARF3*, but instead require misregulation of additional polarity targets of AS1-AS2. Similarly, the synergistic loss of *TAS3A* transcription occurs in response to ectopic ARF3/ARF4 expression, but only when AS1-AS2 activity is simultaneously compromised. In this paradigm, however, the contribution that AS1-AS2 makes is mechanistically distinct (see above).

Double mutants for the AS and ta-siRNA pathways also show a previously unappreciated convergence at leaf complexity. While links between adaxial-abaxial polarity and leaf complexity have been noted (Kim et al., 2003; Yifhar et al., 2012), our data indicate that altered adaxial-abaxial patterning is unlikely to drive this phenotype. Much like the examples described above, the increase in leaf complexity derives from the misregulation of their shared target *ARF3* and the presence of additional factor(s) normally repressed by AS1-AS2. Candidates of particular interest include the AS1-AS2 target *YAB5*, which promotes outgrowth at the leaf margin (Sarojam et al., 2010); KAN1, which physically interacts with ARF3 (Kelley et al., 2012); and the KNOX targets, which already have a well-established role in compound leaf development (Bharathan et al., 2002; Hay et al., 2006; Barkoulas et al., 2008). Interestingly, reduced auxin signaling deepens serrations of *as1* leaves in a *BP*-dependent manner (Hay et al., 2006). When considered in the light of our data, it is thus possible that complexity emerges from the intersection of ARF3-dependent repression of auxin signaling and KNOX gene activity at the margins of developing leaves.

At what point during compound leaf development might intersection of AS1-AS2 target(s), like the KNOX genes, and *ARF3* occur? Increases to leaf complexity derive from PIN1-generated auxin maxima found along the margin of developing primordia whose positioning is achieved, at least in part, through a combination of CUC2 and Aux/IAA activity (Barkoulas et al., 2008; Koenig and Sinha 2010; Bilsborough et al., 2011). As *ARF3* requires polar auxin transport to mediate its effect on leaflet formation, and PIN1-GFP localization is unchanged in *sgs3*, *ARF3* is unlikely to act at this point in the pathway. Once auxin maxima are positioned, isolation of outgrowth is reinforced through the activities of CUC2 and RCO, which repress rates of cell division in flanking regions (Koenig and Sinha 2010; Bilsborough et al., 2011; Sicard et al., 2014; Vlad et al., 2014), presenting another point where *ARF3* may play its role. However, *ARF3* is expressed throughout the developing outgrowth, rather than at its base, and does not affect leaf dissection when overexpressed in isolation, consistent with a different mode of action than either CUC2 or RCO. Instead, we propose that *ARF3*, in conjunction with additional AS pathway targets, promotes organogenic potential at marginal auxin maxima, such that its prolonged activity results in elaboration of serrations into leaflets. Such a role for *ARF3* may be evolutionarily conserved, as hypomorphic mutations in ta-siRNA biogenesis components in tomato (*Solanum lycopersicum*) can condition mild increases in leaf complexity (Yifhar et al., 2012). Thus, our analyses show that the shared repression of *ARF3* by the AS and ta-siRNA pathways intersects with multiple additional AS1-AS2 targets to affect discrete nodes in leaf development.

Taken together with its effects on *MIR166A*, *YAB5*, and *TAS3A*, this study illustrates the surprisingly multifaceted contribution of AS1-AS2 to leaf development, showing that, in conjunction with the ta-siRNA pathway, these transcription factors affect adaxial-abaxial polarity as well as leaf complexity, thereby keeping the Arabidopsis leaf both flat and simple.

METHODS

Plant Materials and Growth Conditions

Plants were grown at 22°C under long-day conditions in soil or on 1% agarose plates containing 1× Murashige and Skoog medium supplemented

with 1% sucrose. Media was supplemented with 5 μM β-estradiol (Sigma-Aldrich) or 5 μM NPA (Sigma-Aldrich) as detailed in the text. The *sgs3-1*, *arf3-2*, and *arf4-2* mutant alleles were isolated in the Col-0 background, while the *as2-4* allele was identified in the En-2 background and introgressed into Col-0 (Guo et al., 2008). The *TAS3A* gene trap line was identified in the Landsberg *erecta* background (GT19682; Garcia et al., 2006); its pattern of expression was not affected by crossing into Col-0. All other transgenic lines were created in the Col-0 background, including *OlexA:AS2-YFP*, *AS1:AS1-HA*, *ARF3:ARF3mut*, *ARF3:ARF3-GUS*, and *PIN1:PIN1-GFP*, which have been previously described (Benková et al., 2003; Fahlgren et al., 2006; Guo et al., 2008; Lodha et al., 2013). The *MIR166A:GUS* and *FIL:GUS* lines were created by fusing 2.5- and 2.4-kb promoter fragments of *MIR166A* and *FIL*, respectively, upstream of the *uidA* gene in the binary vector pKGWFS7 (Karimi et al., 2002). To create the *MIR166AΔ:GUS* construct, a 340-bp fragment upstream of Motif I was joined to the 2.2-kb fragment downstream of Motif II via overlapping PCR and cloned into pKGWFS7. Cloning primers are listed in Supplemental Table 2.

ChIP Assays

ChIP assays were performed as previously described (Guo et al., 2008; Lodha et al., 2013), except magnetic Protein A Dynabeads (Invitrogen) were used in place of agarose Protein A beads. The following antibodies were used: IgG (Abcam ab46540), anti-GFP (Invitrogen A-11122), anti-HA (Abgent AM1008a), anti-histone H3 (Millipore 05-928), and antitrimethyl-histone H3 lysine 27 (Millipore 17-622). ChIP and input DNA samples were assayed by qPCR using iQ SYBR Green Supermix (Bio-Rad) or semi-quantitative PCR using Ex-Taq (Takara). All experiments were performed at least three independent times, and PCR was performed in duplicate. Relative enrichments were calculated as previously described (Lodha et al., 2013), and Student's *t* test was used to calculate statistical significance. Primer sequences are listed in Supplemental Tables 3 and 4.

RT-PCR Analyses

Total RNA was extracted from 12-d-old dissected leaves or apices using Trizol reagent (Gibco BRL). One microgram of RNA was primed with oligo (dT) and reverse transcribed using the SuperScript III first-strand synthesis kit (Invitrogen). For quantitative RT-PCR analysis, relative quantification values were calculated based on at least three biological replicates using the $2^{-\Delta Ct}$ method, with the ΔCt of *ACT2* as normalization control. Wild-type values were set to one and mutant values plotted. Primer sequences are listed in Supplemental Table 5.

Histology and Microscopy

GUS analyses were performed as previously described (Chitwood et al., 2009), using the following concentrations of supplemented ferro/ferricyanide: 10 mM for *MIR166A:GUS*, 6 mM for *FIL:GUS*, 2 mM for the *TAS3A* gene trap line, and 0.5 mM for *ARF3:ARF3-GUS*. Whole-mount seedlings were imaged on a Nikon SMZ1500 dissecting microscope. Sections were imaged on a Leica DM RB compound microscope. For scanning electron microscopy analyses, 12-d-old plants and the leaves of 37-d-old plants were fixed in 4% glutaraldehyde (EMS) for 24 h, followed by a 1% osmium tetroxide (EMS) treatment for 24 h, and then dehydrated using an ethanol series and critical point dried. Material was hand-dissected, sputter-coated twice with gold particles, and imaged with a 15-keV electron beam using a Hitachi S-3500N scanning electron microscope. For PIN1-GFP analyses, leaves of *PIN1:PIN1-GFP* seedlings were dissected and imaged using an LSM 710 confocal microscope.

Accession Numbers

Sequence data from this article can be found in the Arabidopsis Genome Initiative database under the following accession numbers: *AS1*, At2g37630; *AS2*, At1g65620; *MIR166A*, At2g46685; *YAB5*, At2g26580; *ARF3*, At2g33860; and *TAS3A*, At3g17185.

Supplemental Data

Supplemental Figure 1. Promoter regions of polarity determinants occupied by AS2 are also bound by AS1.

Supplemental Figure 2. AS1-AS2 controls the expression domain of its direct target *MIR166A*.

Supplemental Figure 3. No enrichment of H3K27me3 is detected at *ARF3*.

Supplemental Figure 4. *ARF3* expression is detectable in outgrowths on *as2 sgs3* leaves and correlates with the degree of leaf dissection.

Supplemental Figure 5. *as2 sgs3* outgrowths are presaged by PIN1-GFP foci.

Supplemental Figure 6. PIN1-GFP activity persists in leaves of *as2* and *as2 sgs3* seedlings.

Supplemental Table 1. Sequences and locations of AS1-AS2 Motifs I and II.

Supplemental Table 2. Primer pairs used in *promoter:GUS* fusion constructs.

Supplemental Table 3. Primer pairs used in AS2-YFP and AS1-HA ChIP assays.

Supplemental Table 4. Primer pairs used in H3K27me3 ChIP analysis.

Supplemental Table 5. Primers used for quantitative RT-PCR.

ACKNOWLEDGMENTS

We thank Mengjuan Guo, Marcela Carmona, William Kruesi, Marie DeClerck, and Olga Minkina for technical assistance, Tim Mulligan for plant care, and members of the Timmermans lab for helpful ideas and comments that have strengthened the manuscript. We also thank Cris Kuhlemeier for the *PIN1:PIN1-GFP* line and James Carrington for the *ARF3:ARF3mut* and *ARF3:ARF3-GUS* lines. A.Y.H. thanks Blackford for being there when the data were not. A.H.B. was supported by an HFSP long-term postdoctoral fellowship (LT000739/2012-L) and is currently funded through a Marie Curie International Outgoing Fellowship (FP7-PEOPLE-2011-IOF/301610). Work on leaf polarity in the Timmermans lab is supported by grants from the National Science Foundation (IBN-0615752 and IOS-1355018).

AUTHOR CONTRIBUTIONS

A.Y.H., A.H.B., F.T.S.N., and M.C.P.T. designed the project and experiments. A.Y.H., A.H.B., F.T.S.N., and M.L. performed the experiments. A.Y.H. and M.C.P.T. wrote the manuscript.

Received May 20, 2015; revised October 16, 2015; accepted November 2, 2015; published November 20, 2015.

REFERENCES

Angel, A., Song, J., Dean, C., and Howard, M. (2011). A Polycomb-based switch underlying quantitative epigenetic memory. Nature **476:** 105–108.

Barkoulas, M., Hay, A., Kougioumoutzi, E., and Tsiantis, M. (2008). A developmental framework for dissected leaf formation in the *Arabidopsis* relative *Cardamine hirsuta.* Nat. Genet. **40:** 1136–1141.

Benková, E., Michniewicz, M., Sauer, M., Teichmann, T., Seifertová, D., Jürgens, G., and Friml, J. (2003). Local, efflux-dependent auxin gradients as a common module for plant organ formation. Cell **115:** 591–602.

Bharathan, G., Goliber, T.E., Moore, C., Kessler, S., Pham, T., and Sinha, N.R. (2002). Homologies in leaf form inferred from KNOXI gene expression during development. Science **296:** 1858–1860.

Biggin, M.D. (2011). Animal transcription networks as highly connected, quantitative continua. Dev. Cell **21:** 611–626.

Bilsborough, G.D., Runions, A., Barkoulas, M., Jenkins, H.W., Hasson, A., Galinha, C., Laufs, P., Hay, A., Prusinkiewicz, P., and Tsiantis, M. (2011). Model for the regulation of *Arabidopsis thaliana* leaf margin development. Proc. Natl. Acad. Sci. USA **108:** 3424–3429.

Chapman, E.J., and Carrington, J.C. (2007). Specialization and evolution of endogenous small RNA pathways. Nat. Rev. Genet. **8:** 884–896.

Chitwood, D.H., Nogueira, F.T.S., Howell, M.D., Montgomery, T.A., Carrington, J.C., and Timmermans, M.C.P. (2009). Pattern formation via small RNA mobility. Genes Dev. **23:** 549–554.

Emery, J.F., Floyd, S.K., Alvarez, J., Eshed, Y., Hawker, N.P., Izhaki, A., Baum, S.F., and Bowman, J.L. (2003). Radial patterning of *Arabidopsis* shoots by class III *HD-ZIP* and *KANADI* genes. Curr. Biol. **13:** 1768–1774.

Eshed, Y., Baum, S.F., Perea, J.V., and Bowman, J.L. (2001). Establishment of polarity in lateral organs of plants. Curr. Biol. **11:** 1251–1260.

Fahlgren, N., Montgomery, T.A., Howell, M.D., Allen, E., Dvorak, S.K., Alexander, A.L., and Carrington, J.C. (2006). Regulation of *AUXIN RESPONSE FACTOR3* by *TAS3* ta-siRNA affects developmental timing and patterning in *Arabidopsis.* Curr. Biol. **16:** 939–944.

Franco-Zorrilla, J.M., López-Vidriero, I., Carrasco, J.L., Godoy, M., Vera, P., and Solano, R. (2014). DNA-binding specificities of plant transcription factors and their potential to define target genes. Proc. Natl. Acad. Sci. USA **111:** 2367–2372.

Garcia, D., Collier, S.A., Byrne, M.E., and Martienssen, R.A. (2006). Specification of leaf polarity in Arabidopsis via the trans-acting siRNA pathway. Curr. Biol. **16:** 933–938.

Guo, M., Thomas, J., Collins, G., and Timmermans, M.C. (2008). Direct repression of KNOX loci by the ASYMMETRIC LEAVES1 complex of *Arabidopsis.* Plant Cell **20:** 48–58.

Hay, A., Barkoulas, M., and Tsiantis, M. (2006). ASYMMETRIC LEAVES1 and auxin activities converge to repress *BREVIPEDICELLUS* expression and promote leaf development in *Arabidopsis.* Development **133:** 3955–3961.

Hay, A., and Tsiantis, M. (2006). The genetic basis for differences in leaf form between *Arabidopsis thaliana* and its wild relative *Cardamine hirsuta.* Nat. Genet. **38:** 942–947.

Heisler, M.G., Ohno, C., Das, P., Sieber, P., Reddy, G.V., Long, J.A., and Meyerowitz, E.M. (2005). Patterns of auxin transport and gene expression during primordium development revealed by live imaging of the *Arabidopsis* inflorescence meristem. Curr. Biol. **15:** 1899–1911.

Huang, T., Harrar, Y., Lin, C., Reinhart, B., Newell, N.R., Talavera-Rauh, F., Hokin, S.A., Barton, M.K., and Kerstetter, R.A. (2014). *Arabidopsis* KANADI1 acts as a transcriptional repressor by interacting with a specific *cis*-element and regulates auxin biosynthesis, transport, and signaling in opposition to HD-ZIPIII factors. Plant Cell **26:** 246–262.

Hunter, C., Willmann, M.R., Wu, G., Yoshikawa, M., de la Luz Gutiérrez-Nava, M., and Poethig, S.R. (2006). Trans-acting siRNA-mediated repression of *ETTIN* and *ARF4* regulates heteroblasty in *Arabidopsis.* Development **133:** 2973–2981.

Husbands, A., Bell, E.M., Shuai, B., Smith, H.M., and Springer, P.S. (2007). LATERAL ORGAN BOUNDARIES defines a new family of DNA-binding transcription factors and can interact with specific bHLH proteins. Nucleic Acids Res. **35:** 6663–6671.

Husbands, A.Y., Chitwood, D.H., Plavskin, Y., and Timmermans, M.C.P. (2009). Signals and prepatterns: new insights into organ polarity in plants. Genes Dev. **23:** 1986–1997.

Iwakawa, H., Iwasaki, M., Kojima, S., Ueno, Y., Soma, T., Tanaka, H., Semiarti, E., Machida, Y., and Machida, C. (2007). Expression of the *ASYMMETRIC LEAVES2* gene in the adaxial domain of *Arabidopsis* leaves represses cell proliferation in this domain and is critical for the development of properly expanded leaves. Plant J. **51:** 173–184.

Iwasaki, M., et al. (2013). Dual regulation of *ETTIN* (*ARF3*) gene expression by AS1-AS2, which maintains the DNA methylation level, is involved in stabilization of leaf adaxial-abaxial partitioning in *Arabidopsis.* Development **140:** 1958–1969.

Juarez, M.T., Kui, J.S., Thomas, J., Heller, B.A., and Timmermans, M.C.P. (2004). MicroRNA-mediated repression of *rolled leaf1* specifies maize leaf polarity. Nature **428:** 84–88.

Karimi, M., Inzé, D., and Depicker, A. (2002). GATEWAY vectors for Agrobacterium-mediated plant transformation. Trends Plant Sci. **7:** 193–195.

Kelley, D.R., Arreola, A., Gallagher, T.L., and Gasser, C.S. (2012). ETTIN (ARF3) physically interacts with KANADI proteins to form a functional complex essential for integument development and polarity determination in Arabidopsis. Development **139:** 1105–1109.

Kerstetter, R.A., Bollman, K., Taylor, R.A., Bomblies, K., and Poethig, R.S. (2001). *KANADI* regulates organ polarity in *Arabidopsis.* Nature **411:** 706–709.

Kim, M., McCormick, S., Timmermans, M., and Sinha, N. (2003). The expression domain of *PHANTASTICA* determines leaflet placement in compound leaves. Nature **424:** 438–443.

Koenig, D., and Sinha, N. (2010). Evolution of leaf shape: a pattern emerges. In Plant Development, M.C.P. Timmermans, ed (San Diego, CA: California Academic Press), pp. 169–183.

Lang, Y.Z., Zhang, Z.J., Gu, X.Y., Yang, J.C., and Zhu, Q.S. (2004). A physiological and ecological effect of crimpy leaf character in rice (*Oryza sativa* L.) II. Photosynthetic character, dry mass production and yield forming. Acta Agron. Sin. **30:** 883–887.

Lin, W.C., Shuai, B., and Springer, P.S. (2003). The *Arabidopsis LATERAL ORGAN BOUNDARIES*-domain gene *ASYMMETRIC LEAVES2* functions in the repression of *KNOX* gene expression and in adaxial-abaxial patterning. Plant Cell **15:** 2241–2252.

Lodha, M., Marco, C.F., and Timmermans, M.C. (2013). The ASYMMETRIC LEAVES complex maintains repression of KNOX homeobox genes via direct recruitment of Polycomb-repressive complex2. Genes Dev. **27:** 596–601.

Luo, M., Yu, C.W., Chen, F.F., Zhao, L., Tian, G., Liu, X., Cui, Y., Yang, J.Y., and Wu, K. (2012). Histone deacetylase HDA6 is functionally associated with AS1 in repression of KNOX genes in *Arabidopsis.* PLoS Genet. **8:** e1003114.

Marin, E., Jouannet, V., Herz, A., Lokerse, A.S., Weijers, D., Vaucheret, H., Nussaume, L., Crespi, M.D., and Maizel, A. (2010). miR390, Arabidopsis *TAS3* tasiRNAs, and their *AUXIN RESPONSE FACTOR* targets define an autoregulatory network quantitatively regulating lateral root growth. Plant Cell **22:** 1104–1117.

McConnell, J.R., Emery, J., Eshed, Y., Bao, N., Bowman, J., and Barton, M.K. (2001). Role of *PHABULOSA* and *PHAVOLUTA* in determining radial patterning in shoots. Nature **411:** 709–713.

Merelo, P., Xie, Y., Brand, L., Ott, F., Weigel, D., Bowman, J.L., Heisler, M.G., and Wenkel, S. (2013). Genome-wide identification of KANADI1 target genes. PLoS One **8:** e77341.

Moon, J., and Hake, S. (2011). How a leaf gets its shape. Curr. Opin. Plant Biol. **14:** 24–30.

Nakata, M., Matsumoto, N., Tsugeki, R., Rikirsch, E., Laux, T., and Okada, K. (2012). Roles of the middle domain-specific *WUSCHEL-RELATED HOMEOBOX* genes in early development of leaves in *Arabidopsis.* Plant Cell **24:** 519–535.

Ng, K.H., Yu, H., and Ito, T. (2009). *AGAMOUS* controls *GIANT KILLER*, a multifunctional chromatin modifier in reproductive organ patterning and differentiation. PLoS Biol. **7:** e1000251.

Nogueira, F.T.S., Madi, S., Chitwood, D.H., Juarez, M.T., and Timmermans, M.C.P. (2007). Two small regulatory RNAs establish opposing fates of a developmental axis. Genes Dev. **21:** 750–755.

Ori, N., Eshed, Y., Chuck, G., Bowman, J.L., and Hake, S. (2000). Mechanisms that control knox gene expression in the *Arabidopsis* shoot. Development **127:** 5523–5532.

Pekker, I., Alvarez, J.P., and Eshed, Y. (2005). Auxin response factors mediate *Arabidopsis* organ asymmetry via modulation of *KANADI* activity. Plant Cell **17:** 2899–2910.

Rast, M.I., and Simon, R. (2012). *Arabidopsis* JAGGED LATERAL ORGANS acts with ASYMMETRIC LEAVES2 to coordinate KNOX and PIN expression in shoot and root meristems. Plant Cell **24:** 2917–2933.

Reinhart, B.J., Liu, T., Newell, N.R., Magnani, E., Huang, T., Kerstetter, R., Michaels, S., and Barton, M.K. (2013). Establishing a framework for the Ad/abaxial regulatory network of *Arabidopsis*: ascertaining targets of class III homeodomain leucine zipper and KANADI regulation. Plant Cell **25:** 3228–3249.

Reinhardt, D., Frenz, M., Mandel, T., and Kuhlemeier, C. (2005). Microsurgical and laser ablation analysis of leaf positioning and dorsoventral patterning in tomato. Development **132:** 15–26.

Reinhardt, D., Pesce, E.R., Stieger, P., Mandel, T., Baltensperger, K., Bennett, M., Traas, J., Friml, J., and Kuhlemeier, C. (2003). Regulation of phyllotaxis by polar auxin transport. Nature **426:** 255–260.

Roudier, F., et al. (2011). Integrative epigenomic mapping defines four main chromatin states in *Arabidopsis.* EMBO J. **30:** 1928–1938.

Sarojam, R., Sappl, P.G., Goldshmidt, A., Efroni, I., Floyd, S.K., Eshed, Y., and Bowman, J.L. (2010). Differentiating *Arabidopsis* shoots from leaves by combined YABBY activities. Plant Cell **22:** 2113–2130.

Semiarti, E., Ueno, Y., Tsukaya, H., Iwakawa, H., Machida, C., and Machida, Y. (2001). The *ASYMMETRIC LEAVES2* gene of *Arabidopsis thaliana* regulates formation of a symmetric lamina, establishment of venation and repression of meristem-related homeobox genes in leaves. Development **128:** 1771–1783.

Sicard, A., Thamm, A., Marona, C., Lee, Y.W., Wahl, V., Stinchcombe, J.R., Wright, S.I., Kappel, C., and Lenhard, M. (2014). Repeated evolutionary changes of leaf morphology caused by mutations to a homeobox gene. Curr. Biol. **24:** 1880–1886.

Siegfried, K.R., Eshed, Y., Baum, S.F., Otsuga, D., Drews, G.N., and Bowman, J.L. (1999). Members of the YABBY gene family specify abaxial cell fate in Arabidopsis. Development **126:** 4117–4128.

Skopelitis, D.S., Husbands, A.Y., and Timmermans, M.C. (2012). Plant small RNAs as morphogens. Curr. Opin. Cell Biol. **24:** 217–224.

Sussex, I.M. (1951). Experiments on the cause of dorsiventrality in leaves. Nature **167:** 651–652.

Tiwari, S.B., Hagen, G., and Guilfoyle, T. (2003). The roles of auxin response factor domains in auxin-responsive transcription. Plant Cell **15:** 533–543.

Vlad, D., et al. (2014). Leaf shape evolution through duplication, regulatory diversification, and loss of a homeobox gene. Science **343:** 780–783.

Waites, R., and Hudson, A. (1995). *phantastica*: a gene required for dorsoventrality of leaves in *Antirrhinum majus.* Development **121:** 2143–2154.

Williams, L., Carles, C.C., Osmont, K.S., and Fletcher, J.C. (2005). A database analysis method identifies an endogenous trans-acting short-interfering RNA that targets the *Arabidopsis ARF2, ARF3,* and *ARF4* genes. Proc. Natl. Acad. Sci. USA **102**: 9703–9708.

Wu, G., Lin, W.C., Huang, T., Poethig, R.S., Springer, P.S., and Kerstetter, R.A. (2008). KANADI1 regulates adaxial-abaxial polarity in Arabidopsis by directly repressing the transcription of *ASYMMETRIC LEAVES2.* Proc. Natl. Acad. Sci. USA **105:** 16392–16397.

Xu, L., Yang, L., Pi, L., Liu, Q., Ling, Q., Wang, H., Poethig, R.S., and Huang, H. (2006). Genetic interaction between the *AS1-AS2* and *RDR6-SGS3-AGO7* pathways for leaf morphogenesis. Plant Cell Physiol. **47:** 853–863.

Yadav, R.K., Tavakkoli, M., Xie, M., Girke, T., and Reddy, G.V. (2014). A high-resolution gene expression map of the *Arabidopsis* shoot meristem stem cell niche. Development **141:** 2735–2744.

Yang, J.Y., Iwasaki, M., Machida, C., Machida, Y., Zhou, X., and Chua, N.H. (2008). betaC1, the pathogenicity factor of TYLCCNV, interacts with AS1 to alter leaf development and suppress selective jasmonic acid responses. Genes Dev. **22:** 2564–2577.

Yao, X., Wang, H., Li, H., Yuan, Z., Li, F., Yang, L., and Huang, H. (2009). Two types of *cis*-acting elements control the abaxial epidermis-specific transcription of the *MIR165a* and *MIR166a* genes. FEBS Lett. **583:** 3711–3717.

Yifhar, T., Pekker, I., Peled, D., Friedlander, G., Pistunov, A., Sabban, M., Wachsman, G., Alvarez, J.P., Amsellem, Z., and Eshed, Y. (2012). Failure of the tomato trans-acting short interfering RNA program to regulate *AUXIN RESPONSE FACTOR3* and *ARF4* underlies the wiry leaf syndrome. Plant Cell **24:** 3575–3589.

Zhang, G.H., Xu, Q., Zhu, X.D., Qian, Q., and Xue, H.W. (2009). SHALLOT-LIKE1 is a KANADI transcription factor that modulates rice leaf rolling by regulating leaf abaxial cell development. Plant Cell **21:** 719–735.

Zhang, X., Clarenz, O., Cokus, S., Bernatavichute, Y.V., Pellegrini, M., Goodrich, J., and Jacobsen, S.E. (2007). Whole-genome analysis of histone H3 lysine 27 trimethylation in *Arabidopsis.* PLoS Biol. **5:** e129.